forests

MDPI

Article

Surface-Based Analysis of Leaf Microstructures for Adsorbing and Retaining Capability of Airborne Particulate Matter in Ten Woody Species

Myeong Ja Kwak [1], Jong Kyu Lee [1], Sanghee Park [1], Handong Kim [1], Yea Ji Lim [1], Keum-Ah Lee [1], Joung-a Son [2], Chang-Young Oh [2], Iereh Kim [1] and Su Young Woo [1,*]

[1] Department of Environmental Horticulture, University of Seoul, Seoul 02504, Korea; 016na8349@hanmail.net (M.J.K.); gpl90@naver.com (J.K.L.); parksanghee0930@gmail.com (S.P.); blasterkhd92@gmail.com (H.K.); oxll2l@naver.com (Y.J.L.); lka830815@gmail.com (K.-A.L.); a20751385@gmail.com (I.K.)

[2] Urban Forests Research Center, National Institute of Forest Science, Seoul 02455, Korea; jason2015@korea.kr (J.-a.S.); happyohcy@korea.kr (C.-Y.O.)

* Correspondence: wsy@uos.ac.kr; Tel.: +82-10-3802-5242

Received: 15 July 2020; Accepted: 28 August 2020; Published: 29 August 2020

Abstract: We evaluated surface-based analysis for assessing the possible relationship between the microstructural properties and particulate matter (i.e., two size fractions of $PM_{2.5}$ and PM_{10}) adsorption efficiencies of their leaf surfaces on ten woody species. We focused on the effect of PM adsorption capacity between micro-morphological features on leaf surfaces using a scanning electron microscope and a non-contact surface profiler as an example. The species with higher adsorption of PM_{10} on leaf surfaces were Korean boxwood (*Buxus koreana* Nakai ex Chung & al.) and evergreen spindle (*Euonymus japonicus* Thunb.), followed by yulan magnolia (*Magnolia denudata* Desr.), Japanese yew (*Taxus cuspidata* Siebold & Zucc.), Japanese horse chestnut (*Aesculus turbinata* Blume), retusa fringetree (*Chionanthus retusus* Lindl. & Paxton), maidenhair tree (*Ginkgo biloba* L.), and royal azalea (*Rhododendron schlippenbachii* Maxim.). There was a higher capacity for the adsorption of $PM_{2.5}$ on the leaf surfaces of *B. koreana* and *T. cuspidata*, followed by *A. turbinata*, *C. retusus*, *E. japonicus*, *G. biloba*, and *M. denudata*. In wax layer tests, *T. cuspidata*, *A. turbinata*, *R. schlippenbachii*, and *C. retusus* showed a statistically higher $PM_{2.5}$ capturing capacity than the other species. Different types of trichomes were distributed on the adaxial and abaxial leaves of *A. turbinata*, *C. retusus*, *M. denudata*, pagoda tree (*Styphnolobium japonicum* (L.) Schott), *B. koreana*, and *R. schlippenbachii*; however, these trichomes were absent on both sides of the leaves of *G. biloba*, tuliptree (*Liriodendron tulipifera* L.), *E. japonicus*, and *T. cuspidata*. Importantly, leaf surfaces of *G. biloba* and *S. japonicum* with dense or thick epicuticular leaf waxes and deeper roughness revealed lower PM adsorption. Based on the overall performance of airborne PM capture efficiency, evergreen species such as *B. koreana*, *T. cuspidata*, and *E. japonicus* showed the best results, whereas *S. japonicum* and *L. tulipifera* had the lowest capture. In particular, evergreen shrub species showed higher $PM_{2.5}$ depositions inside the inner wall of stomata or the periphery of guard cells. Therefore, in leaf microstructural factors, stomatal size may be related to notably high $PM_{2.5}$ holding capacities on leaf surfaces, but stomatal density, trichome density, and roughness had a limited effect on PM adsorption. Finally, our findings indicate that surface-based microstructures are necessarily not a correlation for corresponding estimates with leaf PM adsorption.

Keywords: leaf microstructure; leaf surfaces; PM_{10}; $PM_{2.5}$; PM adsorption; trichome; roughness

1. Introduction

Particulate matter (PM) is an air pollutant in urban and industrial areas and PM fractions with a diameter of 10 μm or less often exceed air quality standards and cause serious concerns on ecosystems and humans including a wide range of respiratory and vascular diseases [1–4]. Recently, PM abatement technologies have become a global issue, and technological developments for purifying and improving air quality are rapidly expanding in Asia, North America, and Europe [5–8]. Expanding tree canopies across a city is very helpful for adsorbing PM particles and reducing air pollution to improve the urban environment [4]. Optimizing the configuration of greenspace in urban and peri-urban zones that have limited availability for open spaces needs the selection of suitable species that can maximize PM removal. Currently, ambient $PM_{2.5}$ (aerodynamic diameter ≤2.5 μm) and PM_{10} levels (aerodynamic diameter ≤10 μm) exceed the recommended values in many countries [9], especially with high levels concentrated in big cities. A solution for control of elevated PM episodes creates enormous scientific challenges as well as imposes economic costs [10]. Reducing PM emissions that come from vehicles or industrial operations is not an economically viable solution in highly urbanized areas. Plants have been proposed as a sustainable way of reducing artificial PM in urban environments, and they can effectively improve air quality by adsorbing PM_{10} onto leaf surfaces or encapsulating $PM_{2.5}$ within the wax layer [3]. The ability of plants to retain fine particulates depends on the species, leaf and branch density, and surface properties related to the microstructure of leaves [11].

The potential removal of PM by trees for improving urban air quality has been widely mentioned in the literature as one of several benefits of trees in urban environments. In more detail, leaves with deep grooves and high stomatal density were found to have a strong influence on PM retention, and species with regularly arranged stomata may have poor PM retention ability [4]. Thus, the adsorption efficiency of fine dust particles varies depending on macro-morphology and micro-morphology such as trichomes and grooves on leaves of individual trees. Leaves are the main photosynthetic organs with distinctive upper (adaxial) and lower surfaces (abaxial), and the outermost surfaces are covered by a thin continuous layer of lipid material (<0.1–10 μm) called epicuticular wax of an amorphous, crystalline, or semi-crystalline structure [12–14]. Cuticular wax plays an important role in physio-ecological functions by acting as a barrier against abiotic and biotic stress [15]. The quantity and composition of leaf microstructures such as cuticular wax vary widely across plant species and depend upon stresses [16]. According to a recent study, PM induces the overproduction of reactive oxygen species (ROS) and has a direct effect on oxidative stress because of interaction with the lipid layer of the cell membrane [17–21].

The main function of leaf microstructures is to prevent water loss from leaf surfaces, and it also serves as the first barrier for the penetration of biomaterials. Trichomes act as a biochemical defensive role because of the secretion of phenolic compounds, primarily flavonoids, and have protective roles because of their physical properties as single or multicellular epidermal appendages [22,23]. In particular, these microstructures on leaf surfaces provide a site for the adsorption and absorption of air particulates; however, they show different tolerances or sensitivities to pollutants and also differ greatly in their specific affinity for and capture capacity of pollutants [24,25]. PM deposition onto leaf surfaces can markedly induce the possibility of stomatal blocking and photosynthetic inhibition [26,27]. Nevertheless, most recent previous results deal with coupling the presence of complex leaf shape, large surface area, or trichomes (projecting structures on the epidermal surfaces) that can improve particle adsorption capacity [2,11]. Therefore, a detailed understanding of the causal relationships between the unique microstructures and the PM adsorption feedback on different leaf surfaces is important for improving air quality. The main objective of this research focused on assessing and comparing a detailed description of microstructures linked to enhanced adsorption removal of PM in tree species using surface-based analysis techniques.

2. Materials and Methods

2.1. Study Site Description

An urban forest park, the Seoul Forest Park, located in Seoul, South Korea, has been chosen as a study area (37°32.6′ N, 127°2.4′ E; Figure 1). According to annual average concentrations of PM_{10} and $PM_{2.5}$ in Seoul over the past five years [28], PM_{10} and $PM_{2.5}$ concentrations in the Seoul Forest Park were 47.4 μg/m^3 and 24.4 μg/m^3, respectively. These figures are similar to the annual average concentrations of PM_{10} (45.4 μg/m^3) and $PM_{2.5}$ (24.6 μg/m^3) in Seoul as a whole and thereby adequately represent Seoul's air quality. As of 2018, the annual averages of PM_{10} and $PM_{2.5}$ in Seoul were 40 μg/m^3 and 23 μg/m^3 [28], which were two times higher than the Air Quality Guidelines (AQGs) of the World Health Organization's (WHO) recommendations. Importantly, the number of occurrences of "Unhealthy" or "Very unhealthy" in which 24 h mean $PM_{2.5}$ concentrations in Seoul exceeds 35 μg/m^3 tends to last longer than five days.

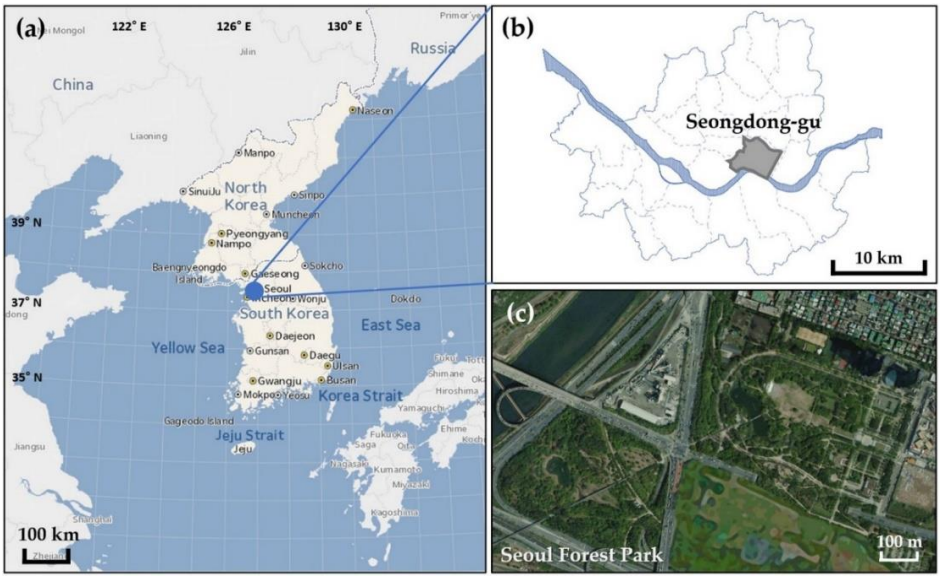

Figure 1. Schematic diagram of a sampling site in Seoul, South Korea (National Geographic Information Institute): (**a**) Korea; (**b**) Seoul sampling site; and (**c**) Seoul Forest Park (digital map image).

2.2. Plant Material and Sample Collection

The Seoul Forest Park is the first one, which is managed by the Citizen group as the public-private partnership under a contract with Seoul Metropolitan Government and the park consists mainly of Japanese horse chestnut (*Aesculus turbinata* Blume), retusa fringetree (*Chionanthus retusus* Lindl. & Paxton), maidenhair tree (*Ginkgo biloba* L.), tuliptree (*Liriodendron tulipifera* L.), yulan magnolia (*Magnolia denudata* Desr.), pagoda tree (*Styphnolobium japonicum* (L.) Schott), Japanese yew (*Taxus cuspidata* Siebold & Zucc.), Korean boxwood (*Buxus koreana* Nakai ex Chung & al.), evergreen spindle (*Euonymus japonicus* Thunb.), and royal azalea (*Rhododendron schlippenbachii* Maxim.) (Table 1). Seven tree species and three shrub species in the Seoul Forest Park were selected as a target species for on-site monitoring during the growing season. We collected n = 200 twigs of each species from branches located in the four-quadrant directions at a tree height of 3 to 6 m from a total of n = 50 individual trees at the Seoul Forest Park. The sampled twigs were placed in a plastic bag and placed in an icebox. After sample processing, all samples collected from the sites were immediately transferred to the laboratory. To explore PM remobilization on leaves as affected by rainfall, leaf sampling was conducted four times during the rainy spell in summer. In particular, we observed the cumulative rainfall of 75 mm, 605 mm, 107 mm, and 52 mm, respectively, for 20 days before four sampling times between July and September 2019.

Table 1. List of ten major species (n = 50) sampled at the Seoul Forest Park in Seoul, Korea with scientific name, common name, family, height, and type (Quoted from: Korea National Arboretum).

Scientific Name	Common Name	Family	Height	Diameter at Breast Height	Type
Aesculus turbinata	Japanese Horse Chestnut	Sapindaceae	10.1 m	29 cm	Deciduous broadleaf tree
Buxus koreana	Korean boxwood	Buxaceae	0.8 m	–	Evergreen broadleaf shrub
Chionanthus retusus	Retusa fringetree	Oleaceae	8.9 m	15.1 cm	Deciduous broadleaf tree
Euonymus japonicus	Evergreen spindle	Celastraceae	1.2 m	6.2 cm	Evergreen broadleaf shrub
Ginkgo biloba	Maidenhair Tree	Ginkgoaceae	12.4 m	15.7 cm	Deciduous conifer tree
Liriodendron tulipifera	Tuliptree	Magnoliaceae	11.0 m	21.3 cm	Deciduous broadleaf tree
Magnolia denudata	Yulan Magnolia	Magnoliaceae	8.0 m	14 cm	Deciduous broadleaf tree
Rhododendron schlippenbachii	Royal azalea	Ericaceae	1.0 m	–	Deciduous broadleaf shrub
Styphnolobium japonicum	Pagoda tree	Leguminosae	11.1 m	22.9 cm	Deciduous broadleaf tree
Taxus cuspidata	Japanese yew	Taxaceae	3.8 m	8.5 cm	Evergreen coniferous shrub or small tree

Note: (–) denotes shrub species. For five individuals of each woody species, the height and diameter at breast height measurements were determined using a digital dendrometer (Criterion™ RD1000, Laser Technology, Centennial, CO, USA) with a laser distance meter (Leica DISTO™ A5; Leica Geosystems, Heerbrugg, Switzerland).

2.3. Determination of PM_{10} and $PM_{2.5}$ Adsorption Capacity on Leaf Surfaces

The amounts of PM_{10} and $PM_{2.5}$ adsorbed on leaf surfaces (namely surface PM_{10} and surface $PM_{2.5}$, respectively) were analyzed by the method of [1]. Leaf samples for quantitative analysis were randomly selected from the branches and transferred to the laboratory. The collected leaves were placed in a glass bottle filled with 250 mL of deionized water, and then ultrasonically cleaned for 1 min using an ultrasonic cleaner (HSt Powersonic 620, Hwashin Technology Company, Seoul, Korea). The pore size of the filters for the eluent was sequentially 10 μm (Nylon filter; Merck Millipore, Darmstadt, Germany), 3 μm (Mixed cellulose ester (MCE) filter; Merck Millipore, Darmstadt Germany), and 0.2 μm (MCE filter; Merck Millipore, Darmstadt, Germany). The weight W_1 (g) of each quantitative filter paper was measured in advance before filtration. After filtration, the filter paper was dried for 24 h at a constant temperature and humidity (temperature 20~25 °C, humidity 35%), and the weight W_2 (g) after filtration was measured. The weight of PM_{10} and $PM_{2.5}$ adsorbed on the surface of the filter for each species was calculated using the difference between the filter weight before filtration of the eluent and the filter weight after filtration (W_2–W_1). The leaf area (cm^2) of the leaves used for the quantitative analysis of fine dust was determined and the amount of fine dust per unit area (mg/m^2) calculated.

2.4. Determination of $PM_{2.5}$ Adsorption Capacity in Epicuticular Wax Layers

PM particles accumulated and encapsulated to leaf wax layers were designated as "in wax PM". Quantification of $PM_{2.5}$ encapsulated in epicuticular wax layers of leaf samples was carried out by the modified method of [1] as shown in Figure 2. By washing the leaf samples that had been rinsed with deionized water in 150 mL of chloroform for 40 s, the epicuticular wax layer was dissolved and PM particles embedded in waxes were removed. Subsequently, the residual was vacuum filtered through a sequential extraction procedure with 10 μm, 3 μm, and 0.2 μm polytetrafluoroethylene (PTFE) filters (Advantec Co., Ltd., Tokyo, Japan) to filter $PM_{2.5}$ particles that originate from epicuticular waxes. Each PTFE filter was initially weighed prior to the membrane filtration process (W_3, g). After the filtration process, the filters were dried in a thermo-hygrostat incubator (25 °C/35% RH) for 24 h and then weighed (W_4, g). Quantification of $PM_{2.5}$ accumulated in the wax layer was calculated by subtracting (W_4–W_3) the weight prior to filtration process (W_3) from the weight after the filtration process (W_4). Then, to obtain the normalized value expressed in mg/m^2, the amount of $PM_{2.5}$ was determined by dividing the filtering weight by the leaf area of each species.

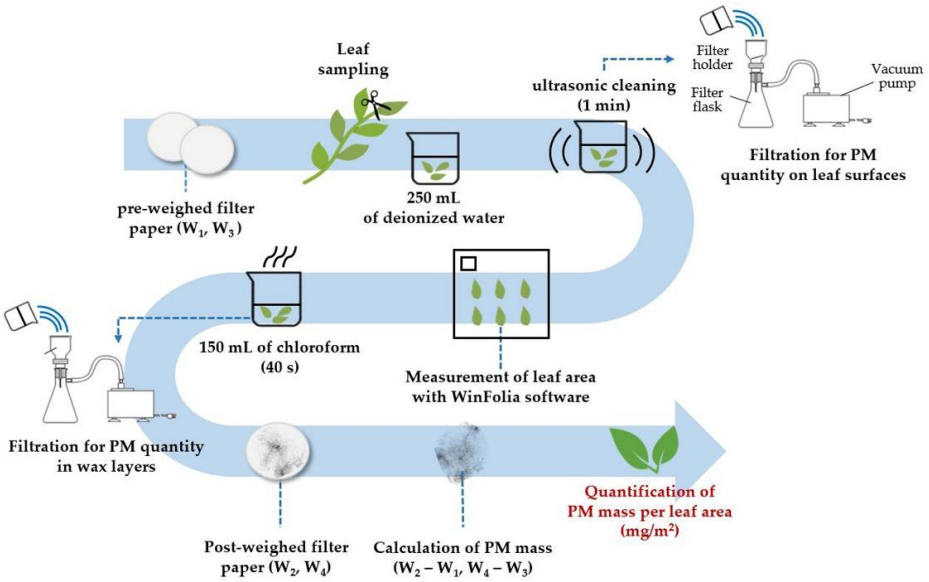

Figure 2. Schematic diagram for quantitative analysis of particulate matter (PM) adsorption using a solid suspension filtering apparatus. W_1, W_2, W_3, and W_4 denote the weight of each quantitative filter paper, the weight of the filter paper dried for 24 h after filtration, the weight of initial each PTFE filter paper, and the weight of the PTFE filter paper dried for 24 h after filtration, respectively.

2.5. Micro-Morphological Characteristics on Leaf Surfaces

For micro-morphological features of leaf surfaces, the sampled 3 to 5 leaves were dried using a freeze dryer and transferred to the Center for Research Facilities at the University of Seoul for surface structure observation. The freeze-dried leaf samples were fragmented into 1 mm × 1 mm, then they were placed on a metal stub and coated with platinum. Leaf micro-morphological characteristics on leaf adaxial and abaxial surfaces (such as surface roughness, stomatal density and size, trichome morphology, and trichome size and density) were observed and imaged to analyze differences among species using a scanning electron microscope (Field emission scanning electron microscopy, FESEM; SU8010, Hitachi High-Tech, Tokyo, Japan). The numbers of trichome and stomata per image were scored, and the size of trichome and guard cell (hereafter referred to as stomatal size; μm) were measured. In addition, the chemical composition of the fine dust adsorbed on the leaf surface was analyzed by energy dispersive X-ray spectroscopy (EDS; Quantax Xflash 6I60, Bruker, Billerica, MA, USA). FESEM-EDS analysis was conducted for assessing the effectiveness of micro-morphological structures in PM deposition and for analyzing the contents of PM-bound elements [29]. After micro-morphological structure observations by the FESEM technique of leaf specimens mounted on a single SEM stub, to further investigate the suitability of surface roughness for adsorbing PM particles, we measured the 3D topography and roughness of leaf surfaces at 50× magnification using a non-contact surface profiler (Bruker Contour GT-K™, Bruker nano GmbH, Berlin, Germany).

2.6. Measurement of the Contact Angle on Leaf Surfaces

The collected leaves were fixed to a slide glass and allowed to air dry to remove moisture, and then 20 μL of ultrapure water for hardwoods or 10 μL of ultrapure water for conifers was dropped using a pipette. Thereafter, the contact angle was analyzed using ImageJ software, an image processing program, for the image photographed under plane conditions.

2.7. Statistical Analysis

All data were statistically analyzed using IBM SPSS Statistics 25 (SPSS Inc., IBM Company Headquarters, Chicago, IL, USA). One-way analysis of variance (ANOVA) and Kruskal–Wallis tests were used to determine statistically significant differences for parametric and non-parametric

continuous variables among independent groups. Statistical comparisons of the roughness on adaxial leaf surfaces were performed using the one-way ANOVA followed by Tukey's post-hoc test. In the Kolmogorov–Smirnov results of the normality test for PM deposition amounts, most of the groups satisfied the usual assumptions of normality, but some groups did not meet the normality of the data. Therefore, the PM deposition differences between test plant species were compared using a non-parametric Kruskal–Wallis rank sum test. Additionally, the Kruskal–Wallis test followed by the Mann–Whitney U test using Bonferroni correction was performed to determine whether the difference in PM adsorption amounts across seasonal rainfall events was statistically significant at a significance level of 0.05. The Pearson's correlation test was calculated based on the average of each variable (surface PM_{10}, surface $PM_{2.5}$, in wax PM_{10}, in wax $PM_{2.5}$, surface roughness, adaxial contact angle, abaxial contact angle, stomatal density, stomatal length, and stomatal width).

3. Results

3.1. Adsorption Capacity on Leaf Surfaces and in Epicuticular Wax Layers

In our study, some variables of PM adsorption amounts do not fulfill normality and therefore the Kruskal–Wallis test was employed. As shown in Figure 3, this indicates that there was statistically significant ($p < 0.001$) among ten species at each PM_{10} and $PM_{2.5}$ adsorbed on leaf surfaces and in the wax layers from major species in Seoul Forest. Effective adsorption of PM_{10} was observed on the leaf surfaces of *Buxus koreana* (72.3 mg/m^2), followed by *Euonymus japonicus* (54.3 mg/m^2), *Taxus cuspidata* (54.1 mg/m^2), *Aesculus turbinata* (49.0 mg/m^2), *Magnolia denudata* (46.7 mg/m^2), *Chionanthus retusus* (40.0 mg/m^2), *Ginkgo biloba* (35.3 mg/m^2), *Rhododendron schlippenbachii* (31.5 mg/m^2), and *Styphnolobium japonicum* (30.5 mg/m^2). Of the species tested, *Liriodendron tulipifera* revealed statistically the lowest value of 27.6 mg/m^2 for the adsorption of PM_{10} particles. The most effective adsorption of $PM_{2.5}$ on leaf surfaces was observed for *Buxus koreana* (26.1 mg/m^2), followed by *Taxus cuspidata* (19.3 mg/m^2), *Aesculus turbinata* (15.1 mg/m^2), *Chionanthus retusus* (12.3 mg/m^2), *Euonymus japonicus* (10.6 mg/m^2), *Ginkgo biloba* (10.4 mg/m^2), *Magnolia denudata* (8.7 mg/m^2), *Liriodendron tulipifera* (8.3 mg/m^2), *Rhododendron schlippenbachii* (7.7 mg/m^2), and *Styphnolobium japonicum* (7.0 mg/m^2).

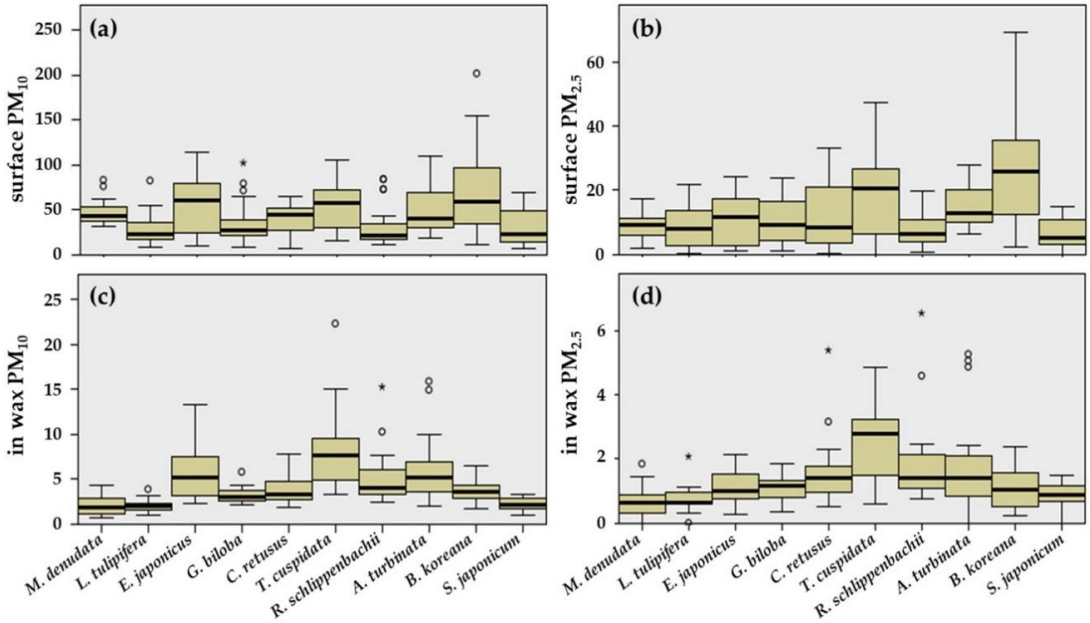

Figure 3. Box-plot of the Kruskal–Wallis rank-sum test for PM particle amounts (mg/m^2) on surface PM_{10}, surface $PM_{2.5}$, wax PM_{10}, and wax $PM_{2.5}$ from leaves of ten plant species growing in the Seoul Forest Park: (**a**) Surface PM_{10}; (**b**) surface $PM_{2.5}$; (**c**) in wax PM_{10}; and (**d**) in wax $PM_{2.5}$. Note: Group differences in PM deposition data were tested using the non-parametric Kruskal–Wallis analysis (n = 20 each group).

Our results showed that there were substantial differences among species for the PM_{10} amount encapsulated in leaf wax layers in the following order (Figure 3): *Taxus cuspidata* (8.4 mg/m^2), *Aesculus turbinata* (6.0 mg/m^2), *Euonymus japonicus* (5.7 mg/m^2), *Rhododendron schlippenbachii* (5.1 mg/m^2), *Chionanthus retusus* (3.7 mg/m^2), *Buxus koreana* (3.6 mg/m^2), *Ginkgo biloba* (3.2 mg/m^2), *Styphnolobium japonicum* (2.2 mg/m^2), *Magnolia denudata* (2.1 mg/m^2), and *Liriodendron tulipifera* (2.0 mg/m^2). With regard to the capacity for adsorption of $PM_{2.5}$ in wax layers, *Taxus cuspidata* was the highest (2.5 mg/m^2), followed by *Aesculus turbinata* (1.8 mg/m^2), *Rhododendron schlippenbachii* (1.8 mg/m^2), *Chionanthus retusus* (1.6 mg/m^2), *Buxus koreana* (1.1 mg/m^2), *Euonymus japonicus* (1.1 mg/m^2), *Ginkgo biloba* (1.1 mg/m^2), *Styphnolobium japonicum* (0.9 mg/m^2), *Magnolia denudata* (0.7 mg/m^2), and *Liriodendron tulipifera* (0.7 mg/m^2). For total PM adsorption for both surfaces and wax layers of leaves (Figure 3), *Buxus koreana* showed the highest amount of PM adsorption (75.9 mg/m^2), followed by *Taxus cuspidata* (62.6 mg/m^2), *Euonymus japonicus* (60.0 mg/m^2), *Aesculus turbinata* (55.0 mg/m^2), *Magnolia denudata* (48.8 mg/m^2), *Chionanthus retusus* (43.7 mg/m^2), *Ginkgo biloba* (38.5 mg/m^2), *Rhododendron schlippenbachii* (36.5 mg/m^2), *Styphnolobium japonicum* (32.7 mg/m^2), and *Liriodendron tulipifera* (29.6 mg/m^2).

Four rainfall events differences in PM adsorption amounts were tested using Kruskal–Wallis tests, followed by the post hoc Mann–Whitney U test with Bonferroni correction (Table 2). Interestingly, PM adsorption amounts of the plants during the seasonal rainfall events were found to be statistically significant differences as follows: Surface PM_{10} (Chi-square test, $X^2 = 91.089$, $p < 0.001$), surface $PM_{2.5}$ ($X^2 = 94.998$, $p < 0.001$), in wax PM_{10} ($X^2 = 14.294$, $p = 0.003$), and in wax $PM_{2.5}$ ($X^2 = 13.101$, $p = 0.004$). In the results of post hoc multiple comparisons with Bonferroni correction, using the Mann–Whitney U test, the variable PM adsorption was mainly affected by the rainy spell in summer (especially in August), except for "in wax $PM_{2.5}$".

Table 2. Post hoc multiple comparisons with Bonferroni correction, using the Mann–Whitney U test of PM adsorption amount of leaves during the four rainfall events.

Particulate Matter	Kruskal Wallis Test			Seasonal Rainfall Events	Mann-Whitney U			
	Chi-Square	Df	*p* Value		*U*	Z	Asymp. Sig.	Significant Difference
Surface PM_{10}	91.089	3	<0.001	July–Aug.	223.0	−7.080	0.000	Yes
				July–Sep.	839.0	−2.833	0.005	Yes
				July–Oct.	1015.0	−1.620	0.105	No
				Aug.–Sep.	331.0	−6.335	0.000	Yes
				Aug.–Oct.	90.0	−7.997	0.000	Yes
				Sep.–Oct.	609.0	−4.419	0.000	Yes
Surface $PM_{2.5}$	94.998	3	<0.001	July–Aug.	280.0	−6.687	0.000	Yes
				July–Sep.	636.0	−4.233	0.000	Yes
				July–Oct.	758.0	−3.392	0.001	Yes
				Aug.–Sep.	794.0	−3.144	0.002	Yes
				Aug.–Oct.	117.0	−7.811	0.000	Yes
				Sep.–Oct.	258.0	−6.839	0.000	Yes
In wax PM_{10}	14.294	3	0.003	July–Aug.	818.0	−2.978	0.003	Yes
				July–Sep.	849.0	−2.764	0.006	Yes
				July–Oct.	761.0	−3.371	0.001	Yes
				Aug.–Sep.	1216.5	−0.231	0.817	No
				Aug.–Oct.	1198.0	−0.358	0.720	No
				Sep.–Oct.	1159.5	−0.624	0.533	No
In wax $PM_{2.5}$	13.101	3	0.004	July–Aug.	877.0	−2.571	0.010	No
				July–Sep.	1006.5	−1.679	0.093	No
				July–Oct.	761.0	−3.371	0.001	Yes
				Aug.–Sep.	1069.0	−1.248	0.212	No
				Aug.–Oct.	1179.5	−0.486	0.627	No
				Sep.–Oct.	976.5	−1.885	0.059	No

Note: The results were determined to be significant if the *p*-value < 0.05/6, i.e., 0.0083, according to Bonferroni correction ($n = 20$). Abbreviations: Df, degrees of freedom; *U*, test statistic for the Mann-Whitney U Test; *Z*, z-score (standard score); Asymp. Sig., asymptotic significance (*p* value).

The results of estimating any subsequent dislodgement of PM adsorbed on leaf surfaces during the rainy season showed that PM on leaf surfaces after rainfall events was higher than before rainfall events (Figure 4a,c). The rainy spell in summer led to increased adsorption of the PM_{10} and $PM_{2.5}$ on leaf surfaces, especially the substantial PM deposition of almost 350% and 300% for *Styphnolobium japonicum* and *Rhododendron schlippenbachii*, respectively (Figure 4a). *Chionanthus retusus* exhibited tremendously enhanced performance by 1000% in $PM_{2.5}$ capture after the summer rainy spell (Figure 4c).

The wash-off patterns by rainfall events of PM_{10} and $PM_{2.5}$ embedded in the wax layer were shown in Figure 4b,d. Importantly, PM_{10} and $PM_{2.5}$ amounts in epicuticular waxes decreased after the rainy spell in summer at the end of July, mainly due to both rainfall duration and intensity. The higher wash-off effects were detected for PM_{10} embedded within the leaf waxes of *Aesculus turbinata* and *Rhododendron schlippenbachii* with a decrease of 71% and 55%. Moreover, these species exhibited a remarkable reduction of 76% and 61%, respectively, for "in wax $PM_{2.5}$". Importantly, *Buxus koreana* exhibited quite similar temporal patterns of PM_{10} accumulation in wax layers during four months (Figure 4b), existing strong encapsulation of PM_{10} in their leaf waxes and *Taxus cuspidata* showed significantly higher capture levels for all PM size fractions in its wax layers throughout the experiment (Figure 4b,d).

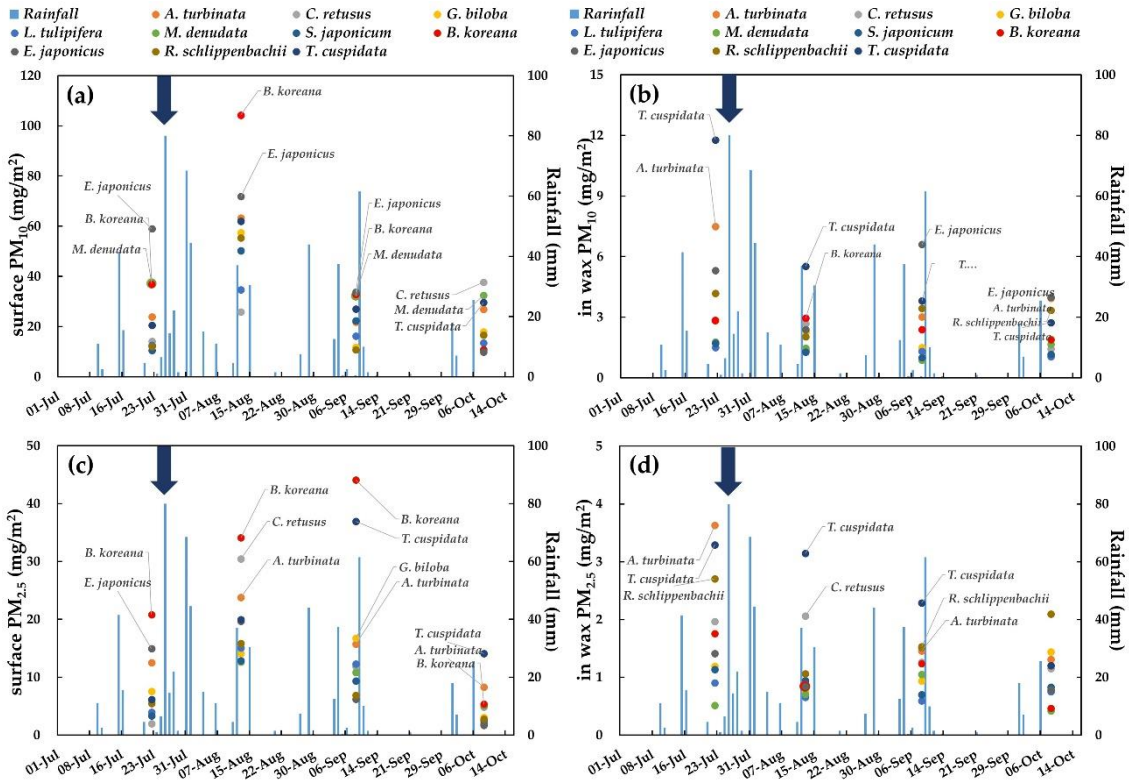

Figure 4. Monthly variations of PM particle amounts (mg/m^2) accumulated both on leaf surfaces and in epicuticular wax layers of ten tree species at the Seoul Forest Park during seasonal rainfall events in Seoul, Korea: (**a**) Surface PM_{10}; (**b**) in wax PM_{10}; (**c**) surface $PM_{2.5}$; and (**d**) in wax $PM_{2.5}$. Note: Arrows indicate the onset of the summer rainy season.

To better understand the removal efficiency of fine dust in the air by individual trees, the quantitative comparative analysis of PM_{10} and $PM_{2.5}$ adsorbed on leaf surfaces and $PM_{2.5}$ encapsulated in the wax layer is required according to the micro-morphological characteristics of the leaves. Ternary Plots are used in many scientific fields to characterize systems based on three values (ratios) of numeric variables, and are tertiary plots or triangular diagrams showing the location of each item in a triangle.

The three peaks in this study represent PM_{10}, $PM_{2.5}$ adsorbed on the leaf surface and $PM_{2.5}$ adsorbed on the wax layer, respectively. It is a diagram based on the ratio of surface PM_{10}/surface $PM_{2.5}$/in wax $PM_{2.5}$ which shows the histological tendency in which fine dust adsorption efficiency is observed in individual trees and can be used to analyze the fine dust adsorption efficiency. This can be effective in improving the selection of the best species for reducing fine dust in urban planting plans by the complete and accurate estimation of fine dust removal of individual trees by the Ternary Plot (Figure 5).

In the ternary plot, among ten major species in Seoul Forest, the high adsorption efficiency of PM_{10} on the leaf surfaces were *Buxus koreana*, *Euonymus japonicus*, and *Magnolia denudata*. The species with high $PM_{2.5}$ adsorption efficiency on the leaf surface were *Buxus koreana*, *Taxus cuspidata*, and *Aesculus turbinata*. On the other hand, *Taxus cuspidata*, *Rhododendron schlippenbachii*, *Aesculus turbinata*, and *Chionanthus retusus* were the best species with high $PM_{2.5}$ mass in the wax layer.

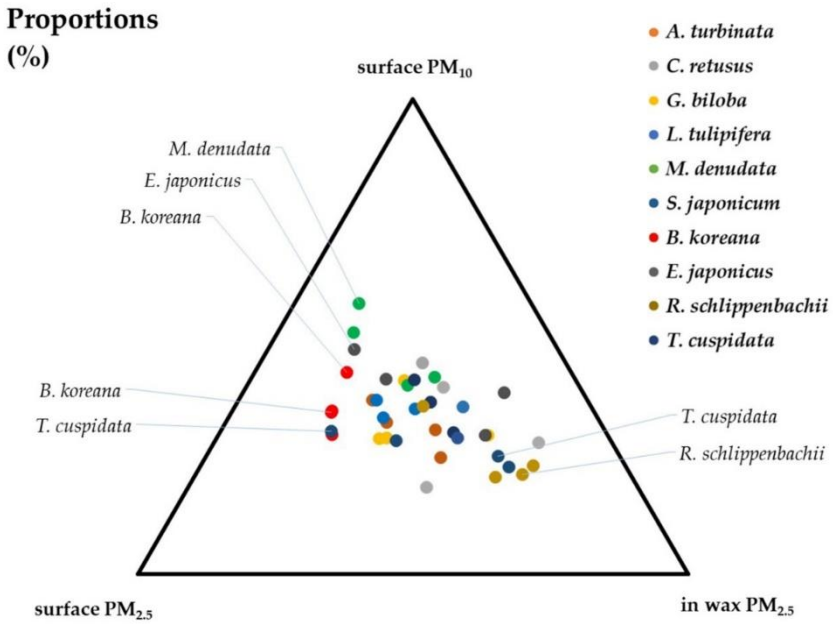

Figure 5. Proportions of surface PM_{10}, surface $PM_{2.5}$, and wax $PM_{2.5}$ captured on leaf surfaces plotted in the ternary diagram (n = 200).

3.2. Micro-Morphological Characteristics on Leaf Surfaces

To confirm the important support of PM removal efficiency based on micromorphological characteristics, micromorphological characteristics such as leaf trichomes, stomata, and epidermal cells were observed in detail using a FESEM (Figures 6–8). Various types of trichomes such as glandular trichomes, non-glandular trichomes, and stellate trichomes were observed on the adaxial and abaxial leaf surfaces of *Aesculus turbinata*, *Chionanthus retusus*, *Magnolia denudata*, *Styphnolobium japonicum*, *Buxus koreana*, and *Rhododendron schlippenbachii* (Figure 6).

These plants showed various types of superficial structure properties linking PM adsorption of trichomes. On the other hand, no trichome development was shown in *Ginkgo biloba*, *Liriodendron tulipifera*, *Euonymus japonicus*, and *Taxus cuspidata*. *Buxus koreana* showed smooth leaf surfaces with very few glandular trichomes on the adaxial vein surfaces (Figure 6a). *Aesculus turbinata* displayed microsurfaces with protuberances along the trichome length (Figure 6b). *Magnolia denudata* showed non-glandular trichomes with smooth surfaces on abaxial leaf surfaces (Figure 6c). *Chionanthus retusus* showed the distribution of two types of the trichome, the peltate glandular and non-glandular, on the leaf abaxial surfaces (Figure 6d). *Rhododendron schlippenbachii* showed non-glandular trichomes with micro- and nano-grooves on abaxial leaf surfaces (Figure 6e). In particular, *Styphnolobium japonicum*

revealed non-glandular trichomes on adaxial and abaxial leaf surfaces, especially showing high stellate (star-shaped) trichomes on adaxial leaf surfaces (Figure 6f).

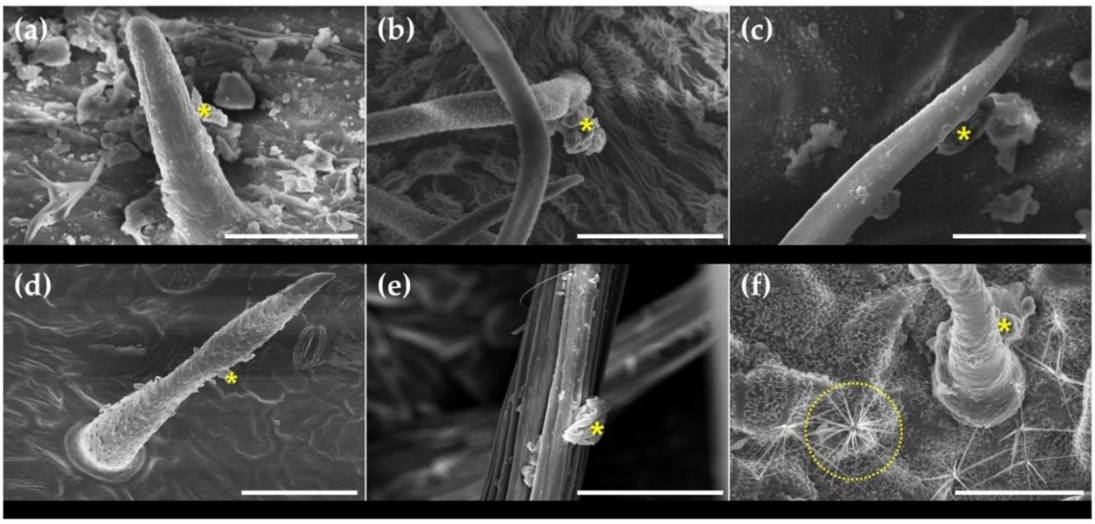

Figure 6. Representative scanning electron microscopy images showing various structural properties of trichomes and PM adsorption on leaf surfaces: (**a**) *Buxus koreana* (glandular trichome on the adaxial surface), (**b**) *Aesculus turbinata* (non-glandular trichome on the abaxial surface), (**c**) *Magnolia denudata* (non-glandular trichome on the abaxial surface), (**d**) *Chionanthus retusus* (peltate glandular and non-glandular trichome on the abaxial surface), (**e**) *Rhododendron schlippenbachii* (non-glandular trichome on the abaxial surface), and (**f**) *Styphnolobium japonicum* (stellate and non-glandular trichomes on the adaxial surface). Note: Yellow asterisk and dotted circle indicate PM particles of different size fractions and stellate trichome, respectively. Scale bars: (**a,c,f**) 30 μm; (**b,d,e**) 50 μm.

As shown in Table 3, *Styphnolobium japonicum* exhibited higher trichome distribution on adaxial and abaxial leaf surfaces, followed by *Aesculus turbinata*, *Chionanthus retusus*, *Magnolia denudata*, and *Rhododendron schlippenbachii*. *Rhododendron schlippenbachii* showed the longest trichome size of 981 μm and 1328 μm, respectively on adaxial and abaxial surfaces, indicating the lowest trichome density of 2 and 3 per mm^2. As shown Figure 6f, the SEM analysis showed that *Styphnolobium japonicum* was abundant as 17 per mm^2, 440 per mm^2, and 48 per mm^2 in non-glandular and stellate trichomes of adaxial leaf surfaces and non-glandular trichome of abaxial leaf surfaces. These non-glandular and stellate trichomes of adaxial leaf surfaces and non-glandular trichome of abaxial leaf surfaces were 213 μm, 33 μm, and 459 μm, respectively.

Besides the micromorphological differences of trichomes, there was a clear difference in stomatal size (Figure 7). In particular, the stomatal size (i.e., guard cell length and width; μm) and density on abaxial leaf surfaces were completely summarized in Table 2. The stomatal density (No. of stomata per mm^2) on abaxial leaf surfaces was greater in *Aesculus turbinata* (637 per mm^2), followed by *Rhododendron schlippenbachii* (347 per mm^2), *Chionanthus retusus* (316 per mm^2), *Magnolia denudata* (275 per mm^2), *Euonymus japonicus* (243 per mm^2), *Taxus cuspidata* (187 per mm^2), *Liriodendron tulipifera* (166 per mm^2), *Buxus koreana* (127 per mm^2), and *Ginkgo biloba* (99 per mm^2). The stomatal length and width were found to have high size of 42 μm long and 33 μm wide, 27 μm long and 21 μm with, and 42 μm long and 34 μm with, respectively, in *Buxus koreana*, *Euonymus japonicus*, and *Taxus cuspidata* (Table 3).

Table 3. Specific leaf micro-morphological characteristics (stomata and trichomes) on adaxial and abaxial leaf surfaces of ten species.

Species	Stomata on Leaf Surfaces			Trichomes on Leaf Surfaces				
	Density (No. mm^{-2})	Size (μm) Length	Size (μm) Width	Trichome Types	Distribution Adaxial	Distribution Abaxial	Size (μm) Adaxial	Size (μm) Abaxial
Aesculus turbinata	637 ± 190	12 ± 3	5 ± 2	non-glandular	–	++		182 ± 108
Chionanthus retusus	316 ± 142	20 ± 3	8 ± 2	non-glandular	–	+		195 ± 75
				peltate glandular	+	++		37 ± 3
Ginkgo biloba	99 ± 8	22 ± 3	15 ± 3		–	–		
Liriodendron tulipifera	166 ± 13	20 ± 5	8 ± 2		–	–		
Magnolia denudata	275 ± 52	15 ± 2	6 ± 1	non-glandular	+	+	192 ± 38	397 ± 76
Styphnolobium japonicum	178 ± 19	12 ± 2	6 ± 2	non-glandular	+	++	213 ± 29	459 ± 141
				stellate	+		33 ± 8	
Buxus koreana	127 ± 9	42 ± 3	33 ± 3	glandular	+	–	54 ± 14	
Euonymus japonicus	243 ± 36	27 ± 1	21 ± 1		–	–		
Rhododendron schlippenbachii	347 ± 35	17 ± 2	8 ± 1	non-glandular	+	+	981 ± 315	1328 ± 428
Taxus cuspidata	187 ± 24	42 ± 4	34 ± 4		–	–		

Note: (–) absence trichomes, (+) a few trichomes, (++) many trichomes.

Moreover, the different PM particle sizes were deposited adjacent to the inner wall of stomata in *Taxus cuspidata* (Figure 7g) and *Buxus koreana* (Figure 7h) or the periphery of guard cells in *Euonymus japonicus* (Figure 7i), considering the size of the stomatal openings. There were high trichomes and epicuticular wax layers on leaf abaxial surfaces of *Styphnolobium japonicum*, which prevented any clear observation of stomata, because of the large amounts of densely distributed epicuticular wax crystals (Figure 7f).

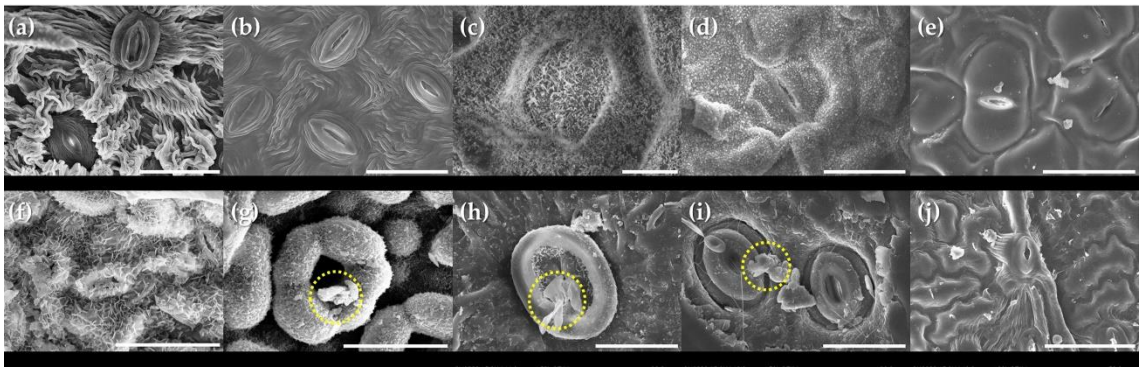

Figure 7. SEM images showing various structural properties of stomata and PM adsorption on abaxial leaf surfaces: (**a**) *Aesculus turbinata*; (**b**) *Chionanthus retusus*; (**c**) *Ginkgo biloba*; (**d**) *Liriodendron tulipifera*; (**e**) *Magnolia denudata*; (**f**) *Styphnolobium japonicum*; (**g**) *Taxus cuspidata*; (**h**) *Buxus koreana*; (**i**) *Euonymus japonicus*; (**j**) *Rhododendron schlippenbachii*. Note: Yellow circles in image denote PM particles of different size fractions adjacent to the inner wall of stomata or the periphery of guard cells. Scale bars: (**c**) 10 μm; (**a**,**b**,**d**,**f**–**i**) 30 μm; (**e**,**j**) 50 μm.

For the determination of sources, formation, and chemical composition of PM_{10} and $PM_{2.5}$ particles on leaf surfaces, EDS spectra of individual particles were obtained by the SEM-EDS analysis (data not shown). Our EDS data showed that the spherical iron (Fe) oxides with trace amounts of aluminum (Al), silicon (Si), calcium (Ca), potassium (K), sodium (Na), and magnesium (Mg) were identified in PM particles adsorbed on adaxial and abaxial leaf surfaces. In particular, we confirmed that the aluminosilicate-type particles were composed of irregular aggregates with the Silicon–Oxygen–Aluminum (Si–O–Al) group from the elemental analysis of the SEM-EDS. The less

abundant heavy metal elements (cadmium and nickel) were found in PM particles on leaf surfaces of major plant species growing in the Seoul Forest Park.

To explore the relationship between the PM adsorption and influencing leaf microstructural factors, we analyzed data on the possible relationship using a Pearson's correlation test. There were no significant correlations between stomatal size and density with any "in wax PM" particles tested. The stomatal size of abaxial leaf surfaces played an important role in the adsorption of surface PM_{10} and $PM_{2.5}$. The surface PM_{10} had a significant positive correlation with stomatal length ($r = 0.711$, $p < 0.05$) and width ($r = 0.741$, $p < 0.05$). The surface $PM_{2.5}$ was a positively strong correlation with stomatal length ($r = 0.808$, $p < 0.01$) and width ($r = 0.794$, $p < 0.01$).

There was no statistically significant relationship between each side contact angle of adaxial and abaxial leaf surfaces and PM adsorption efficiency (data not shown). Furthermore, *Aesculus turbinata*, *Ginkgo biloba*, *Euonymus japonicus*, *Liriodendron tulipifera*, *Styphnolobium japonicum*, and *Taxus cuspidata* were found to have a statistically higher contact angle on abaxial leaf surfaces than on adaxial leaf surfaces, which was attributed to the thicker wax layers on the abaxial surfaces (data not shown).

Next, we looked at the effect of the actual depth of micro-grooves which can be considered as a parameter representing surface roughness using the FESEM technique (Figure 8) and non-contact 3D optical profiler (Figure 9). The 3D topographical variations and leaf surface roughness were measured by the non-contact surface profiler using white light interferometry (Figure 9). The important microfeatures on adaxial leaf surfaces of ten species are grooves and PM particles, which can be seen in Figures 8 and 9. Here, we obtained the FESEM and 3D topographical images at 3000× and 50× magnification encompassing multiple leaf cells to correctly measure the surface roughness. The large area topographical images of *Styphnolobium japonicum* (Figure 9f) and *Rhododendron schlippenbachii* (Figure 9j) even displayed a relatively uniform trichome on adaxial leaf surfaces. *Styphnolobium japonicum* (5.19 μm) showed the highest surface roughness on the adaxial leaves, due to long non-glandular trichomes (Figure 9f).

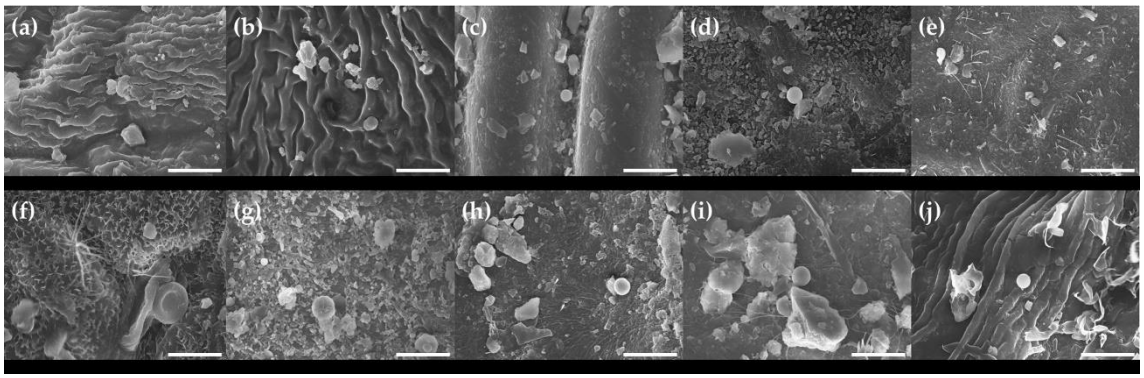

Figure 8. Surface images by utilizing the scanning electron microscope (SEM) on micro-roughness of adaxial leaf surfaces of ten species in urban forests: (**a**) *Aesculus turbinata*; (**b**) *Chionanthus retusus*; (**c**) *Ginkgo biloba*; (**d**) *Liriodendron tulipifera*; (**e**) *Magnolia denudata*; (**f**) *Styphnolobium japonicum*; (**g**) *Taxus cuspidata*; (**h**) *Buxus koreana*; (**i**) *Euonymus japonicus*; (**j**) *Rhododendron schlippenbachii*. Note: Images show different roughness scales, waxes, and PM adsorption conditions on adaxial leaf surfaces. Scale bars: 10 μm.

The mean value of leaf surface roughness was measured on the adaxial side appearing higher PM adsorption from the SEM images on seven tree species and three shrub species (Figure 9k). There were significant roughness differences among species ($p < 0.05$). The adaxial leaf surfaces of *Styphnolobium japonicum* (5.19 μm) showed the roughest surfaces among ten species, followed by *Ginkgo biloba* (3.42 μm), *Rhododendron schlippenbachii* (2.93 μm). The mean roughness values of *Euonymus japonicus*, *Liriodendron tulipifera*, *Aesculus turbinata*, *Taxus cuspidata*, *Magnolia denudata*, *Buxus koreana*, and *Chionanthus retusus* were significantly smaller by 2.04 μm, 1.61 μm, 1.48 μm, 1.36 μm,

1.32 μm, 1.28 μm, and 1.13 μm, respectively than those of the *Styphnolobium japonicum*. Additionally, we found that increase of long non-glandular trichomes in 3D topographical images (representing the leaf roughness) interrupted the surface $PM_{2.5}$ adsorptions, especially showing these properties in *Styphnolobium japonicum* and *Rhododendron schlippenbachii*. By observing the 3D topography and roughness of adaxial leaf surfaces, no significant link was found between the upper roughness and its PM adsorption (data not shown).

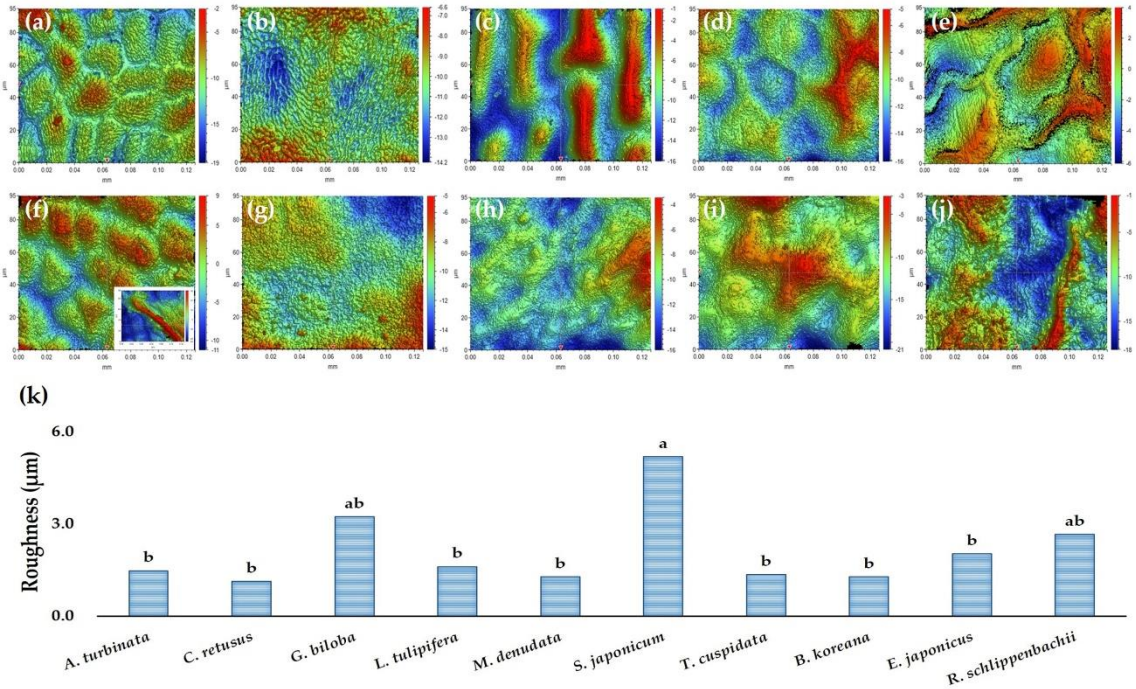

Figure 9. 3D surface topography reconstructions using non-contact surface profiler showing surface roughness on adaxial leaf surfaces: (**a**) *Aesculus turbinata*; (**b**) *Chionanthus retusus*; (**c**) *Ginkgo biloba*; (**d**) *Liriodendron tulipifera*; (**e**) *Magnolia denudata*; (**f**) *Styphnolobium japonicum*; (**g**) *Taxus cuspidata*; (**h**) *Buxus koreana*; (**i**) *Euonymus japonicus*; (**j**) *Rhododendron schlippenbachii*; (**k**) Roughness data among ten species distinguished by microsized structures areas in the replicated surfaces (50× magnification). Note: (**f**) and (**j**) images display long non-glandular trichomes on adaxial leaf surfaces. The same lowercase letters above a bar graph (**k**) represent non-statistically significant differences among species using Tukey's post-hoc analysis with 95% confidence level, $p < 0.05$ ($n = 30$).

4. Discussion

Stomatal shape, density, and distribution observed on the surface of leaves have been studied as important traits in various taxa. Trichomes are largely divided into glandular trichomes and non-glandular trichomes and can be differentiated into different forms and functions depending on plant species [30]. Previous studies have demonstrated that trichomes play a broader role in the interaction between plants and the environment. Although there have been few studies on trichomes in relation to leaf boundary layer resistance and evaporation, recent studies show that they may play a substantial role in leaf–moisture relationships and affect leaf wettability, water retention, and absorption. Trichomes on adaxial and abaxial leaf surfaces can function differently within the same leaf [31]. Various types of trichomes found on adaxial and abaxial leaf surfaces of trees can deposit particles with a size of 2.5–100 μm [30]. The trichomes, a derivative of various leaf epidermal cells, have well-established chemical defense functions as a physical barrier, such as interfering with the movement of insects and herbivores, but non-secretory biomechanical functions have emerged as another prominent strategy for plants. In this study, we accurately described various trichome types of 10 major trees in Seoul Forest. In particular, abundant epicuticular wax micro-structures

on leaf surfaces (e.g., *Ginkgo biloba*) can lead to repeated removal of particles because of continuous water repellency (i.e., leaf hydrophobicity) during the summer rainy season. The self-cleaning leaf surfaces can lead to reduced PM adsorption, thereby affecting PM deposition and accumulation on the leaf surfaces over an entire growing season [12,32,33]. In addition, stomata have a length of 10 to 80 μm and have varying densities of 5 to 1000 (no. mm^{-2}) depending on the plant species and environmental conditions [34,35]. Stomatal size is 46–125 μm^2 [36], so that airborne $PM_{2.5}$ or PM_{10} can be sufficiently adsorbed or embedded around leaf stomata [11,37]; thus, stomata are likely to have several functions for airborne PM reduction as depositional spots. By observing leaf microstructures with a scanning electron microscope, the presence of $PM_{2.5}$ adjacent to the inner wall of stomata or on guard cells was confirmed in leaves of *Buxus koreana, Taxus cuspidata*, and *Euonymus japonicus*. When $PM_{2.5}$ is deposited in the substomatal cavity through stomata, it interferes with the overall photosynthetic process, not only with photosystem II [38]. Therefore, PM adsorbed on leaf surfaces can lead to modification of physico-chemical properties in plants including chlorophyll biosynthesis, resulting in leaf chlorosis. In addition, plant species planted along roadsides showed reduced stomatal size because of PM adsorption without any growth changes; therefore, [19] reported their adsorption potential for PM removal efficiency. Furthermore, the presence of higher grooves and trichomes on leaf surfaces may adsorb some atmospheric particulates and produce a buffering role [39,40] of $PM_{2.5}$-induced stomatal blocking [41]. There is a positive correlation between $PM_{2.5}$ and PM_{10} adsorption within epicuticular waxes and the wax amount [42]; thus, *Styphnolobium japonicum* revealed lower PM adsorption within waxes by having higher trichome density (Figure 6 and Table 2). More specifically, the aerial surfaces of leaves are covered by a waxy cuticle (<0.1–10 μm) as a protective film on adaxial and abaxial surfaces [11]. The main function of the cuticle is as the first barrier to prevent the penetration of biomaterials and to regulate water evaporation from leaf surfaces, and most plant species have specialized unicellular or multicellular trichome structures regarded as derivatives of leaf epidermal cells. Trichomes can also play a role in direct technical defense by their physical properties or indirect biochemical defense by the release of secondary metabolites [11,22].

We identified distinct variations in the detection of PM particle amounts of ten major species during the rainy spell in summer (Figure 4) because of the temporal variability of surface wettability in leaf micromorphological structures [43]. A previous study [44] suggested that a significant negative correlation is found between contact angle and PM capture efficiency on leaf surfaces. Nevertheless, we found that the leaf PM retention amounts were not correlated with the contact angles of droplets on adaxial and abaxial surfaces. PM adsorption increased rapidly after the rainy season compared with before the rainy season (Figure 4). An explanation for this result may be that surface wettability is triggered because of the mechanical or chemical abrasive action of the epidermal wax from high-intensity rainfall events during the rainy season [43]. In addition, evergreen woody shrubs may tend to present low wash-off rates but to retain PM permanently because of hydrophobicity of sticky or waxy leaves during natural rain events [45]. As a result, broad-leaved species may have a stronger $PM_{2.5}$ wash-off process on leaf surfaces by rainfall than coniferous species. Nevertheless, natural rainfall events do not necessarily lead to depressed PM retention performance for leaf surfaces [46,47].

High rain intensity may lead to leaves having a shorter $PM_{2.5}$ accumulation cycle and a higher PM wash-off efficiency [47], resulting in lower efficiency in $PM_{2.5}$ depositions. PM through dry and wet deposition remains adsorbed onto leaf surfaces and may not return from the surfaces to the atmosphere under normal weather conditions [30]. However, although the PM adsorption amounts after the rainy season revealed differences among species, there were no significant seasonal changes. A large number of studies have shown that leaf physical properties, such as shape, trichomes, and stomata, vary considerably depending on the species; and this difference significantly affects PM adsorption and retention capacities [29,39,46,48–52]. As confirmed by SEM images, the $PM_{2.5}$ adsorption capacity was different with differences in the trichome shape, distribution, and density in the leaf epidermis (Figures 6–8). In general, the trichome density appears to be related to $PM_{2.5}$ amounts adsorbed on the leaf surfaces; however, this does not necessarily mean that there is a positive correlation between them.

In the present study, *Buxus koreana* had a relatively high $PM_{2.5}$ removal efficiency, but showing very few trichomes on leaf surfaces based on the SEM images of an individual trichome. Importantly, leaves with protuberances along the trichome length such as those of *Aesculus turbinata* may be helpful in retaining $PM_{2.5}$ [41]. *Magnolia denudata*, which has trichomes with smooth surfaces, was found to retain more PM_{10} than $PM_{2.5}$. A detailed relationship between PM adsorption and roughness on leaf surfaces can be found in previous studies. In general, the roughness of the grooved topographic surfaces can play a positive role in the PM adsorption efficiency of leaf surfaces [53]. However, we found no significant positive correlation between PM adsorption and roughness. In general, the larger leaf roughness was observed on the leaf adaxial surfaces of *Styphnolobium japonicum* (5.19 μm), *Ginkgo biloba* (3.23 μm), and *Rhododendron schlippenbachii* (2.67 μm) (Figure 9 and Table 3). Furthermore, leaf epicuticular wax tends to capture or encapsulate permanently PM because of hydrophobicity [45]; however, several studies have shown that extremely water-repellent adaxial and abaxial surfaces have poor adsorption capacity toward particles during high rainfall conditions [37,40,44].

Meanwhile, *Rhododendron schlippenbachii* was found to adsorb "in wax $PM_{2.5}$" on micro- and nano-grooves of trichome surface structures, but owing to the low trichome density there was no effect on the whole PM adsorption efficiency. It is known that leaves with smooth surfaces, low stomatal densities, and shallow substomatal cavities have a low adsorption efficiency of $PM_{2.5}$. The results showed that the low trichome density of smooth surfaces has poor ability to adsorb $PM_{2.5}$ and that there is also a statistically positive correlation between $PM_{2.5}$ adsorption capacities and many protruding trichomes [54]. Plants could be used potentially as effective adsorbents for microparticles, and leaf micromorphological properties such as roughness, size, grooves, trichomes, and stomata could be positively correlated with PM adsorption and retention. However, another study [50] reported that PM removal efficiencies were negatively correlated with trichome density and length. As mentioned above, plants can play an important role in the prevention and treatment of airborne particulates by adsorbing $PM_{2.5}$ onto the inner wall of stomata or the periphery of guard cells, but there is no correlation between stomatal density and PM adsorption. *Buxus koreana*, *Taxus cuspidata*, and *Euonymus japonicus* indicated high-efficiency of $PM_{2.5}$ removals, but they also showed lower stomatal density and larger stomatal pore size compared with those of other trees. Studies have found that *Euonymus japonicus* is most effective for adsorbing PM on its leaf surfaces [55]. Also, there was a positive correlation between PM adsorption and stomatal size [56]. Previous studies have also reported that a needle leaf tree accumulates more $PM_{2.5}$ than a broad-leaved tree [11,57,58], and the effect of adsorbing PM from these conifers is because of their epicuticular waxes-rich small leaf area [58].

Trees perform overall air quality benefits in urban and suburban areas by mitigating air pollution [59,60]. Also, the selection of high-efficiency tree species for capturing PM particles should be a prerequisite for achieving an appropriate urban forest [50]. As micromorphological epidermis traits, grooves, trichomes, and stomata on the adaxial leaf surfaces of trees play an important role in adsorbing PM re-suspended into the atmosphere during the growing season. Overall, *Buxus koreana*, *Taxus cuspidata*, and *Euonymus japonicus* need to be a priority when choosing urban trees to improve air quality because of the high efficiency of both the inflow of $PM_{2.5}$ within the inner wall of stomata and the adsorption of PM_{10} onto their leaf surfaces. These woody species are mainly evergreen shrubs planted as lower layers in parks and roadsides and have high capacities for adsorbing and retaining PM particles throughout four seasons. According to a previous study, the resuspension of dust deposited around a road affects the PM concentrations in the atmosphere, and the highest PM concentrations are found at a height of 1.2 m from the ground [61].

In particular, PM particles are reportedly composed of heavy metals such as lead (Pb), mercury (Hg), cadmium (Cd), and zinc (Zn) [62,63]; and heavy metal-enriched $PM_{2.5}$ particles can be deposited on leaf surfaces by flows into the atmosphere from industrial processes. Our results confirmed the EDS spectra of individual PM particles that are a wide spectrum of elements with different degrees of toxicity. PM particles can be classified as aluminosilicate/silica mineral, Si–Al rich fly ash, Fe oxide particle, titanium (Ti) dominant particle, sulfate/carbonate crystal, and carbonaceous aerosols as well as

soot, organic carbon, tarball, and irregularly shaped carbon. The Si–Al rich fly ash is mostly spherical with a smooth surface, and it can become agglomerates by combining with other particles. The Si–Al rich fly ash originates from anthropogenic contamination such as fossil fuels, biomass burning, and smelting [64]. Irregularly shaped aluminosilicate/silica minerals are the main types of PM particles observed with a size of approximately 2 μm or more. Silica contains predominantly Si and O without other elements, whereas aluminosilicate particles have more complex compositions including Al, Ca, Fe, K, Mg, Na, and Si. Aluminosilicate and silica are present in the atmosphere by resuspension from sand, road dust, and construction; and they have been identified as important components of many rock types in almost all regions [64]. Furthermore, the spherical Fe-rich particles can be originated artificially in coal boilers, metal industries, and power plants that have different temperature conditions, gradually accumulating on leaf surfaces in the process of soil resuspension.

5. Conclusions

Urban trees are currently being proposed as the only sustainable means to reduce anthropogenic PM in urban environments. Specifically, an increasing number of studies have demonstrated that the ability of plants to adsorb and retain PM depends on species, leaf and branch density, and the microstructural properties of leaf surfaces. We conducted to evaluate urban forest species with excellent adsorption and retention capacity of PM_{10} on leaf surfaces and $PM_{2.5}$ in wax layers through an understanding of the microstructure and physical properties of leaves. A significant difference in airborne PM removal capacity was found among seven tree species and three shrub species. *Buxus koreana*, *Taxus cuspidata*, and *Euonymus japonicus*, evergreen shrubs planted as lower layers on urban forests and roadsides, can have the advantage of being able to adsorb PM throughout four seasons. In particular, *Taxus cuspidata* showed high removal efficiency for PM particles in the wax layer compared to other tree species. Finally, testing for leaf unique microstructures towards interacting with PM adsorption feedback, we found that the ultrastructure of leaves such as surface roughness, trichome, and stomata may not necessarily be a positive or negative correlation with leaf PM adsorption. Nevertheless, the efficiency of PM adsorption is somewhat related to structural properties of grooves, stomata, and trichomes on leaf surfaces, especially the micro- to nano-morphologies of these structures. Additionally, the abaxial trichomes may indicate protective or buffering effects on stomatal aperture against PM particles with a size less than $PM_{2.5}$. Future studies need to be obtained experimentally PM pollutants that might underlie a functional disorder in the photosynthetic apparatus to more firmly establish its causal relationship.

Author Contributions: Conceptualization, S.Y.W.; methodology, M.J.K.; validation, C.-Y.O., J.-a.S., and I.K.; formal analysis, S.P. and J.K.L.; investigation, S.P., H.K., Y.J.L., and K.-A.L.; resources, J.K.L.; data curation, Y.J.L., S.P., H.K., and K.-A.L.; writing—original draft preparation, M.J.K. and J.K.L.; writing—review and editing, M.J.K.; visualization, M.J.K.; supervision, S.Y.W.; project administration, J.K.L.; funding acquisition, S.Y.W. All authors have read and agreed to the published version of the manuscript.

Funding: This study was carried out with the support of 'A Study on Mechanism and Function Improvement of Plants for Reducing Air Pollutants' (Grant No. FE0000-2018-01-2019) from National Institute of Forest Science (NIFoS), Republic of Korea.

Acknowledgments: Special thanks go to the Urban Forests Research Center team, especially Jae Hyoung Cho of Urban Forests Research Center, Forest Conservation Department, National Institute of Forest Science (NIFoS) for suggestions that improved the project. We would also like to thank the Center for Research Facilities at the University of Seoul for the microscope technical support in the experimental field.

Conflicts of Interest: The authors declare no conflict of interest.

References

1. Dzierżanowski, K.; Popek, R.; Gawrońska, H.; Saebø, A.; Gawroński, S.W. Deposition of particulate matter of different size fractions on leaf surfaces and in waxes of urban forest species. *Int. J. Phytoremediat.* **2011**, *13*, 1037–1046. [CrossRef] [PubMed]
2. De Oliveira, M.L.; de Melo, E.J.T.; Miguens, F.C. *Tillandsia stricta* Sol (*Bromeliaceae*) leaves as monitors of airborne particulate matter-A comparative SEM methods evaluation: Unveiling an accurate and odd HP-SEM method. *Microsc. Res. Tech.* **2016**, *79*, 869–879. [CrossRef] [PubMed]
3. Urošević, M.A.; Jovanović, G.; Stević, N.; Deljanin, I.; Nikolić, M.; Tomašević, M.; Samson, R. Leaves of common urban tree species (*Aesculus hippocastanum*, *Acer platanoides*, *Betula pendula* and *Tilia cordata*) as a measure of particle and particle-bound pollution: A 4-year study. *Air Qual. Atmos. Health* **2019**, *12*, 1081–1090. [CrossRef]
4. Liu, L.; Guan, D.; Peart, M.R. The morphological structure of leaves and the dust-retaining capability of afforested plants in urban Guangzhou, South China. *Environ. Sci. Pollut. Res.* **2012**, *19*, 3440–3449. [CrossRef]
5. Kroeger, T.; McDonald, R.I.; Boucher, T.; Zhang, P.; Wang, L. Where the people are: Current trends and future potential targeted investments in urban trees for PM_{10} and temperature mitigation in 27 U.S. cities. *Landsc. Urban. Plan.* **2018**, *177*, 227–240. [CrossRef]
6. Zhai, S.; Jacob, D.J.; Wang, X.; Shen, L.; Li, K.; Zhang, Y.; Gui, K.; Zhao, T.; Liao, H. Fine particulate matter ($PM_{2.5}$) trends in China, 2013–2018: Separating contributions from anthropogenic emissions and meteorology. *Atmos. Chem. Phys.* **2019**, *19*, 11031–11041. [CrossRef]
7. Zhang, X.; Zhang, W.; Yi, M.; Wang, Y.; Wang, P.; Xu, J.; Niu, F.; Lin, F. High-performance inertial impaction filters for particulate matter removal. *Sci. Rep.* **2018**, *8*, 4757. [CrossRef]
8. Weagle, C.L.; Snider, G.; Li, C.; Van Donkelaar, A.; Philip, S.; Bissonnette, P.; Burke, J.; Jackson, J.; Latimer, R.; Stone, E.; et al. Global sources of fine particulate matter: Interpretation of $PM_{2.5}$ chemical composition observed by SPARTAN using a global chemical transport model. *Environ. Sci. Technol.* **2018**, *52*, 11670–11681. [CrossRef]
9. Sosa, B.S.; Porta, A.; Colman Lerner, J.E.; Banda Noriega, R.; Massolo, L. Human health risk due to variations in PM_{10}–$PM_{2.5}$ and associated PAHs levels. *Atmos. Environ.* **2017**, *160*, 27–35. [CrossRef]
10. Zanoletti, A.; Bilo, F.; Borgese, L.; Depero, L.E.; Fahimi, A.; Ponti, J.; Valsesia, A.; Spina, R.L.; Montini, T.; Bontempi, E. SUNSPACE, a porous material to reduce air particulate matter (PM). *Front. Chem.* **2018**, *6*, 534. [CrossRef]
11. Wei, X.; Lyu, S.; Yu, Y.; Wang, Z.; Liu, H.; Pan, D.; Chen, J. Phylloremediation of air pollutants: Exploiting the potential of plant leaves and leaf-associated microbes. *Front. Plant Sci.* **2017**, *8*, 1318. [CrossRef] [PubMed]
12. Neinhuis, C. Characterization and distribution of water-repellent, self-cleaning plant surfaces. *Ann. Bot.* **1997**, *79*, 667–677. [CrossRef]
13. Kirkwood, R.C. Recent developments in our understanding of the plant cuticle as a barrier to the foliar uptake of pesticides. *Pestic. Sci.* **1999**, *55*, 69–77. [CrossRef]
14. Ristic, Z.; Jenks, M.A. Leaf cuticle and water loss in maize lines differing in dehydration avoidance. *J. Plant Physiol.* **2002**, *159*, 645–651. [CrossRef]
15. Jetter, R.; Kunst, L.; Samuels, A.L. Composition of plant cuticular waxes. In *Annual Plant Reviews, Biology of the Plant Cuticle*; Riederer, M., Müller, C., Eds.; Blackwell Publishing: Oxford, UK, 2007; Volume 23, pp. 145–181.
16. Shaheenuzzamn, M.; Liu, T.; Shi, S.; Wu, H.; Wang, Z. Research advances on cuticular waxes biosynthesis in crops: A review. *Int. J. Agric. Biol.* **2019**, *21*, 911–921. [CrossRef]
17. Tian, N.; Liu, F.; Wang, P.; Zhang, X.; Li, X.; Wu, G. The molecular basis of glandular trichome development and secondary metabolism in plants. *Plant Gene* **2017**, *12*, 1–12. [CrossRef]
18. Pandey, S.; Goel, R.; Bhardwaj, A.; Asif, M.H.; Sawant, S.V.; Misra, P. Transcriptome analysis provides insight into prickle development and its link to defense and secondary metabolism in *Solanum viarum* Dunal. *Sci. Rep.* **2018**, *8*, 1–12. [CrossRef] [PubMed]
19. Chaudhary, I.J.; Rathore, D. Suspended particulate matter deposition and its impact on urban trees. *Atmos. Pollut. Res.* **2018**, *9*, 1072–1082. [CrossRef]
20. Badach, J.; Dymnicka, M.; Baranowski, A. Urban Vegetation in Air Quality Management: A Review and Policy Framework. *Sustainability* **2020**, *12*, 1258. [CrossRef]

21. Song, Y.; Maher, B.A.; Li, F.; Wang, X.; Sun, X.; Zhang, H. Particulate matter deposited on leaf of five evergreen species in Beijing, China: Source identification and size distribution. *Atmos. Environ.* **2015**, *105*, 53–60. [CrossRef]
22. Yu, W.; Wang, Y.; Wang, Y.; Li, B.; Liu, Y.; Liu, X. Application of a coupled model of photosynthesis and stomatal conductance for estimating plant physiological response to pollution by fine particulate matter ($PM_{2.5}$). *Environ. Sci. Pollut. Res.* **2018**, *25*, 19826–19835. [CrossRef] [PubMed]
23. Risom, L.; Møller, P.; Loft, S. Oxidative stress-induced DNA damage by particulate air pollution. *Mutat. Res. Fundam. Mol. Mech. Mutagenesis* **2005**, *592*, 119–137. [CrossRef] [PubMed]
24. Øvrevik, J.; Refsnes, M.; Låg, M.; Holme, J.; Schwarze, P. Activation of proinflammatory responses in cells of the airway Mucosa by particulate matter: Oxidant-and non-oxidant-mediated triggering mechanisms. *Biomolecules* **2015**, *5*, 1399–1440. [CrossRef] [PubMed]
25. Rai, P.K. Impacts of particulate matter pollution on plants: Implications for environmental biomonitoring. *Ecotoxicol. Environ. Saf.* **2016**, *129*, 120–136. [CrossRef] [PubMed]
26. Tsai, M.H.; Hsu, L.F.; Lee, C.W.; Chiang, Y.C.; Lee, M.H.; How, J.M.; Wu, C.M.; Huang, C.L.; Lee, I.T. Resveratrol inhibits urban particulate matter-induced COX-2/PGE_2 release in human fibroblast-like synoviocytes via the inhibition of activation of NADPH oxidase/ROS/NF-κB. *Int. J. Biochem. Cell Biol.* **2017**, *88*, 113–123. [CrossRef]
27. Šuškalo, N.; Hasanagić, D.; Topalić-Trivunović, L.; Kukrić, Z.; Samelak, I.; Savić, A.; Kukavica, B. Antioxidative and antifungal response of woody species to environmental conditions in the urban area. *Ecotoxicology* **2018**, *27*, 1095–1106. [CrossRef] [PubMed]
28. National Institute of Environmental Research. Air Quality Monitoring Station; AQMS. Available online: http://www.airkorea.or.kr/web/last_amb_hour_data (accessed on 6 August 2019).
29. Gajbhiye, T.; Pandey, S.K.; Lee, S.S.; Kim, K.H. Size fractionated phytomonitoring of airborne particulate matter (PM)and speciation of PM bound toxic metals pollution through *Calotropis procera* in an urban environment. *Ecol. Indic.* **2019**, *104*, 32–40. [CrossRef]
30. Zampieri, M.C.T.; Sarkis, J.E.S.; Pestana, R.C.B.; Tavares, A.R.; Melo-de-Pinna, G.F.A. Characterization of *Tibouchina granulosa* (Desr.) Cong. (*Melastomataceae*) as a biomonitor of air pollution and quantification of particulate matter adsorbed by leaves. *Ecol. Eng.* **2013**, *61*, 316–327. [CrossRef]
31. Bickford, C.P. Ecophysiology of leaf trichomes. *Funct. Plant Biol.* **2016**, *43*, 807. [CrossRef]
32. Neinhuis, C.; Barthlott, W. Seasonal changes of leaf surface contamination in beech, oak, and ginkgo in relation to leaf micromorphology and wettability. *New Phytol.* **1998**, *138*, 91–98. [CrossRef]
33. Li, Q.; Li, Y.; Zhu, L.; Xing, B.; Chen, B. Dependence of plant uptake and diffusion of polycyclic aromatic hydrocarbons on the leaf surface morphology and micro-structures of cuticular waxes. *Sci. Rep.* **2017**, *7*, 46235. [CrossRef] [PubMed]
34. Hetherington, A.M.; Woodward, F.I. The role of stomata in sensing and driving environmental change. *Nature* **2003**, *424*, 901–908. [CrossRef]
35. Shahinnia, F.; Le Roy, J.; Laborde, B.; Sznajder, B.; Kalambettu, P.; Mahjourimajd, S.; Tilbrook, J.; Fleury, D. Genetic association of stomatal traits and yield in wheat grown in low rainfall environments. *BMC Plant Biol.* **2016**, *16*, 150. [CrossRef] [PubMed]
36. Dow, G.J.; Berry, J.A.; Bergmann, D.C. The physiological importance of developmental mechanisms that enforce proper stomatal spacing in *Arabidopsis thaliana*. *New Phytol.* **2014**, *201*, 1205–1217. [CrossRef] [PubMed]
37. Kwak, M.J.; Lee, J.; Kim, H.; Park, S.; Lim, Y.; Kim, J.E.; Baek, S.G.; Seo, S.M.; Kim, K.N.; Woo, S.Y. The removal efficiencies of several temperate tree species at adsorbing airborne particulate matter in urban forests and roadsides. *Forests* **2019**, *10*, 960. [CrossRef]
38. Shukla, S.; Sharma, R.; Sahu, M. Dust pollution affect morphophysiological traits of plant *Mangifera indica* linn. *Int. J. Bot.* **2019**, *15*, 1–4. [CrossRef]
39. Li, Y.; Wang, S.; Chen, Q. Potential of thirteen urban greening plants to capture particulate matter on leaf surfaces across three levels of ambient atmospheric pollution. *Int. J. Environ. Res. Public Health* **2019**, *16*, 402. [CrossRef]
40. Zhang, Y.; Song, H.; Wang, X.; Zhou, X.; Zhang, K.; Chen, X.; Liu, J.; Han, J.; Wang, A. The roles of different types of trichomes in tomato resistance to cold, drought, whiteflies, and botrytis. *Agronomy* **2020**, *10*, 411. [CrossRef]

41. Li, Y.; Wang, Y.; Wang, B.; Wang, Y.; Yu, W. The response of plant photosynthesis and stomatal conductance to fine particulate matter ($PM_{2.5}$) based on leaf factors analyzing. *J. Plant Biol.* **2019**, *62*, 120–128. [CrossRef]
42. Popek, R.; Gawrońska, H.; Wrochna, M.; Gawroński, S.W.; Sæbø, A. Particulate matter on foliage of 13 woody species: Deposition on surfaces and phytostabilisation in waxes–a 3-year study. *Int. J. Phytoremediat.* **2013**, *15*, 245–256. [CrossRef]
43. Wang, J.; Hu, Z.; Chen, Y.; Chen, Z.; Xu, S. Contamination characteristics and possible sources of PM10 and PM2.5 in different functional areas of Shanghai, China. *Atmos. Environ.* **2013**, *68*, 221–229. [CrossRef]
44. He, X.; Ruan, Y.; Chen, W.; Lu, T. Responses of the anti-oxidative system in leaves of *Ginkgo biloba* to elevated ozone concentration in an urban area. *Bot. Stud.* **2006**, *47*, 409–416.
45. Xu, X.; Xia, J.; Gao, Y.; Zheng, W. Additional focus on particulate matter wash-off events from leaves is required: A review of studies of urban plants used to reduce airborne particulate matter pollution. *Urban For. Urban Green* **2020**, *48*, 126559. [CrossRef]
46. Wang, H.; Shi, H.; Wang, Y. The wetting of leaf surfaces and its ecological significances. In *Wetting and Wettability*; Intech: Rijeka, Croatia, 2015; pp. 295–321. [CrossRef]
47. Xie, C.; Yan, L.; Liang, A.; Che, S. Understanding the washoff processes of $PM_{2.5}$ from leaf surfaces during rainfall events. *Atmos. Environ.* **2019**, *214*, 116844. [CrossRef]
48. Rai, A.; Kulshreshtha, K.; Srivastava, P.K.; Mohanty, C.S. Leaf surface structure alterations due to particulate pollution in some common plants. *Environmentalist* **2010**, *30*, 18–23. [CrossRef]
49. Liu, L.; Fang, Y.M.; Wang, S.C.; Xie, Y.; Yang, D.D. Leaf micro-morphology and features in adsorbing air suspended particulate matter and accumulating heavy metals in seven tress species. *Huanjing Kexue/Environ. Sci.* **2013**, *34*, 2361–2367.
50. Ram, S.S.; Majumder, S.; Chaudhuri, P.; Chanda, S.; Santra, S.C.; Maiti, P.K.; Sudarshan, M.; Chakraborty, A. Plant canopies: Bio-monitor and trap for re-suspended dust particulates contaminated with heavy metals. *Mitig. Adapt. Strateg. Glob. Chang.* **2014**, *19*, 499–508. [CrossRef]
51. Yan, G.; Liu, J.; Zhu, L.; Zhai, J.; Cong, L.; Ma, W.; Wang, Y.; Wu, Y.; Zhang, Z. Effectiveness of wetland plants as biofilters for inhalable particles in an urban park. *J. Clean. Prod.* **2018**, *194*, 435–443. [CrossRef]
52. Baraldi, R.; Chieco, C.; Neri, L.; Facini, O.; Rapparini, F.; Morrone, L.; Rotondi, A.; Carriero, G. An integrated study on air mitigation potential of urban vegetation: From a multi-trait approach to modeling. *Urban For. Urban Green* **2019**, *41*, 127–138. [CrossRef]
53. Shi, J.; Zhang, G.; An, H.; Yin, W.; Xia, X. Quantifying the particulate matter accumulation on leaf surfaces of urban plants in Beijing, China. *Atmos. Pollut. Res.* **2017**, *8*, 836–842. [CrossRef]
54. Zhao, X.; Yan, H.; Liu, M.; Kang, L.; Yu, J.; Yang, R. Relationship between $PM_{2.5}$ adsorption and leaf surface morphology in ten urban tree species in Shenyang, China. *Energy Sources Part A Recover. Util. Environ. Eff.* **2019**, *41*, 1029–1039. [CrossRef]
55. Wang, H.; Shi, H.; Li, Y.; Yu, Y.; Zhang, J. Seasonal variations in leaf capturing of particulate matter, surface wettability and micromorphology in urban tree species. *Front. Environ. Sci. Eng.* **2013**, *7*, 579–588. [CrossRef]
56. Weerakkody, U.; Dover, J.W.; Mitchell, P.; Reiling, K. Evaluating the impact of individual leaf traits on atmospheric particulate matter accumulation using natural and synthetic leaves. *Urban For. Urban Green* **2018**, *30*, 98–107. [CrossRef]
57. Terzaghi, E.; Wild, E.; Zacchello, G.; Cerabolini, B.E.L.; Jones, K.C.; Di Guardo, A. Forest Filter Effect: Role of leaves in capturing/releasing air particulate matter and its associated PAHs. *Atmos. Environ.* **2013**, *74*, 378–384. [CrossRef]
58. Chen, L.; Liu, C.; Zhang, L.; Zou, R.; Zhang, Z. Variation in tree species ability to capture and retain airborne fine particulate matter ($PM_{2.5}$). *Sci. Rep.* **2017**, *7*, 1–11. [CrossRef]
59. Yli-Pelkonen, V.; Scott, A.A.; Viippola, V.; Setälä, H. Trees in urban parks and forests reduce O_3, but not NO_2 concentrations in Baltimore, MD, USA. *Atmos. Environ.* **2017**, *167*, 73–80. [CrossRef]
60. Nowak, D.J.; Hirabayashi, S.; Doyle, M.; McGovern, M.; Pasher, J. Air pollution removal by urban forests in Canada and its effect on air quality and human health. *Urban. For. Urban. Green.* **2018**, *29*, 40–48. [CrossRef]
61. Valotto, G.; Zannoni, D.; Guerriero, P.; Rampazzo, G.; Visin, F. Characterization of road dust and resuspended particles close to a busy road of Venice mainland (Italy). *Int. J. Environ. Sci. Technol.* **2019**, *16*, 6513–6526. [CrossRef]

62. Shahid, M.; Dumat, C.; Niazi, N.K.; Xiong, T.T.; Farooq, A.B.U.; Khalid, S. Ecotoxicology of Heavy Metal(loid)-Enriched Particulate Matter: Foliar Accumulation by Plants and Health Impacts. In *Reviews of Environmental Contamination and Toxicology (Continuation of Residue Reviews)*; Springer: New York, NY, USA, 2019; pp. 1–49.
63. Liu, Z.; Zhou, J.; Zhang, J.; Mao, Y.; Huang, X.; Qian, G. Evaluation for the heavy metal risk in fine particulate matter from the perspective of urban energy and industrial structure in China: A meta-analysis. *J. Clean. Prod.* **2020**, *244*, 118597. [CrossRef]
64. Yin, H.; Mu, S.; Zhao, L.; Qi, X.; Pan, X. Microscopic morphology and elemental composition of size distributed atmospheric particulate matter in Urumqi, China. *Environ. Earth Sci.* **2013**, *69*, 2139–2150. [CrossRef]